Tunable optomechanically induced transparency in double quadratically coupled optomechanical cavities within a common reservoir

C. Bai, B. P. Hou,* D. G. Lai, and D. Wu

College of Physics and Electronic Engineering, Institute of Solid State Physics, Sichuan Normal University, Chengdu 610101, People's Republic of China

(Received 3 September 2015; revised manuscript received 4 February 2016; published 4 April 2016)

We consider the optomechanically induced transparency in the double quadratically coupled optomechanical cavities within a common reservoir, in which the two cavities are driven by the coupling fields. It is shown that the probe transparency is improved by increasing the coupling field (the left coupling field) applied on the probing cavity, but the transparency position (the probe frequency of the maximal transparency) is shifted to high frequency. The coupling field (the right coupling field) applied on the other quadratically coupled cavity can lead to a low-frequency shift for the transparency position, which can be used to fix the transparency position by adjusting the right coupling field. We get the quantitative findings that the transparency position is exactly determined by the intensity difference between the two coupling fields. On the other hand, it is found that when the two coupled optomechanical cavities interact with their common reservoir, the cross decay induced by the common reservoir can improve the probe transparency and widen the transparency window. Finally, the effects of the environment's temperature on the transparency are investigated. This will be useful in cooling the membrane, squeezing and entangling the output fields.

DOI: 10.1103/PhysRevA.93.043804

I. INTRODUCTION

The interaction between electromagnetic radiation and mechanical motion can be realized in the optomechanical system (OMS) by using radiation pressure [1–3]. The OMS has attracted much attention because of its many potential applications, such as in entangling the macroscopic oscillator and the cavity field [4], cooling the mechanical vibrations to their quantum ground states [5–7], and producing the quantum nonlinearities in quantum processing [8–10].

Recently, the optomechanically induced transparency (OMIT), which was originally discovered in the multilevel atomic system by using atomic coherence [11,12], has been demonstrated in the OMS theoretically [13] and experimentally [14,15], respectively. Many studies on OMIT in OMS have been developed in the context of the linearization procedure [13–15]. Subsequently, OMIT with higher-order sidebands [16] and the nonlinear versions of OMIT without the linearization procedure [17–19] were investigated. Manipulation of OMIT in an optomechanical cavity made by two moving mirrors which contain a Kerr-down-conversion nonlinear crystal was also considered [20]. To get much more flexible controllability of OMIT, the investigation of OMIT in single-cavity OMS has been generalized to the case of two-cavity OMS. For example, OMIT and slow light in a two-mode cavity optomechanical system composed of two cavity modes interacting with a common mechanical resonator were theoretically demonstrated [21]. The optomechanically induced absorption (OMIA) in the double-cavity configurations of the hybrid optoelectromechanical systems was predicted [22]. Also, the mechanical-mode splitting of the movable mirror as well as OMIT in the splitting region in the two-mode optomechanical system were investigated [23]. Recently, we have considered the OMIT and OMIA accompanied by normal-mode splitting (NMS) in strongly tunnel-coupled optomechanical cavities [24].

Besides the optomechanical systems with the linear coupling between the optical field and the mechanical mode, there exist quadratically coupled optomechanical systems in which the optical cavity field is coupled parametrically to the square of the position of a mechanical oscillator. The quadratic interaction in an optomechanical system can be realized by placing a membrane at a cavity node (or antinode) of the intracavity modes [25–27]. In the quadratically coupled optomechanical systems, there appear many interesting phenomena, such as the cooling and squeezing of a mechanical oscillator as well as their dependencies on membrane absorption [28,29], basic quantum characteristics [30–32], tunneling of a macroscopic optomechanical membrane [33], single-photon emission and scattering [34], and quantum nonlinearity [35,36]. Recently, the single-mechanical-mode quadratically coupled optomechanical system has been generalized to two- or multiple-mechanical-mode quadratically coupled optomechanics. For example, in such generalized quadratically coupled optomechanical systems the hybridization of the two mechanical modes [37], the optomechanical cooling [38], trapping and entangled-state engineering of vibrational modes [39], and bistability and bifurcations [40] were investigated. On the other hand, the generalized two-optical-mode quadratically coupled optomechanical system has been proposed. A two-color mirror trapping and cooling in a two-cavity quadratically coupled optomechanical system were considered [41], and the tunneling of the photon between the two cavities and the dynamics of the membrane were investigated [42].

In general, the dissipation or decoherence induced by the interaction between the composite quantum system and its surrounding environment devastates the quantum properties in the system. However, when the coupled systems are coupled to a common reservoir, the quantum phenomenon such as entanglement between the subsystems can persist for a long

*bphou@sicnu.edu.cn

time. Therefore, many quantum phenomena in the coupled system within a common reservoir were studied. For example, the coherence phenomenon of two coupled dissipative oscillators within a common reservoir was comprehensively analyzed [43]. And, a decoherence-free subspace in a cavity quantum electrodynamics involving two modes in the presence of a common reservoir was predicted [44]. Subsequently, the dynamics of the entanglement between two oscillators in the same environment was characterized [45]. Recently, the synchronization in quantum networks of harmonic oscillators within a common environment [46] and the heat transport in optomechanical arrays in contact with a common bath [47] were investigated. To our knowledge, the OMIT in the double optomechanical cavities within a common reservoir has not yet been investigated.

Recently, the OMIT and slow light in a single-mode quadratically coupled optomechanical system were demonstrated [48,49]. In such an optomechanical system, the OMIT is improved by increasing the coupling field which deepens and widens the transparency window. However, the probe transparency position, i.e., the probe frequency of the minimum absorption (or maximal transparency) value in the transparency window, is shifted to high frequency with increase of the coupling field. Thus, it is difficult to fix the OMIT position at a certain frequency and simultaneously improve the OMIT by increasing the coupling field. In the present paper, we shall investigate the OMIT in the two-mode quadratically coupled optomechanical system composed by two cavities within a common reservoir, which are independently pumped by the coupling fields. It is found that the probe transparency window becomes deeper and the transparency position is shifted to high frequency with increase of the coupling field (the left coupling field) applied on the probing cavity, while the coupling field (right coupling field) driving the coupled cavity suppresses the transparency and leads to a low-frequency shift for the transparency position. We get the quantitative findings that the transparency position can be exactly determined by the intensity difference between the two coupling fields. Thus the application of the right coupling field on the coupled cavity can overcome the frequency shift of the transparency position in a single-mode quadratically optomechanical system when increasing the coupling field to improve the transparency. Although the right coupling field can assist in fixing the transparency position, it suppresses the OMIT induced by the left coupling field. Subsequently, we consider the OMIT in the two-mode quadratically coupled optomechanical system in which the two cavities are coupled to a common reservoir, and investigate the effects of the cross decay induced by the common reservoir on the OMIT. We find that the cross decay enhances the transparency and widens the transparency window, which can alleviate the suppressions of the OMIT induced by the right coupling field. Additionally, it is found that the temperature of the environment can improve the OMIT in the quadratically coupled optomechanical system.

The paper is organized as follows: In Sec. II we describe the model and solve its dynamical equation. The OMIT as well as its variations with the strengths of the two coupling fields in the double quadratically coupled optomechanical cavities are displayed in Sec. III. The enhancement of the OMIT by the cross decay and the thermal temperature is investigated in Sec. IV. Finally, in Sec. V we summarize our main results.

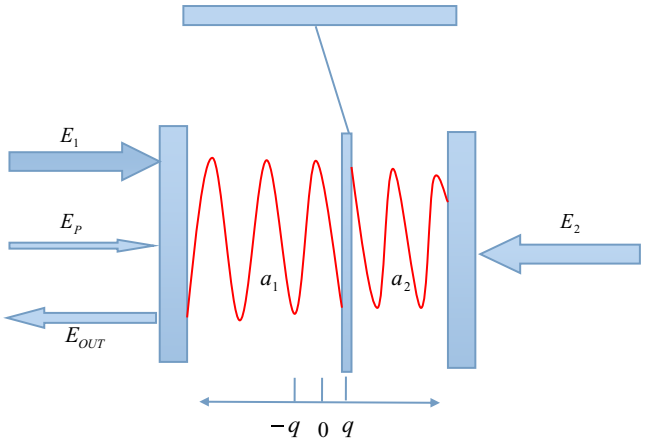

FIG. 1. Sketch of the system. Two cavities are quadratically coupled to the displacement of a membrane suspended in the cavity. The left fixed mirror of the optical cavity is simultaneously driven by a strong coupling field of amplitude E_1 with frequency ω_1 and a weak probe field of amplitude E_p with frequency ω_p. The right fixed mirror in the quadratically coupled optomechanical system is driven by another strong coupling field of amplitude E_2 with frequency ω_2.

II. MODE AND DYNAMICAL EQUATION

Our optomechanical system, which is shown in Fig. 1, consists of two partially transmitting mirrors fixed at $\pm L$, and a membrane oscillating with a very small displacement q around its equilibrium position between the two fixed mirrors. The membrane separates the cavity formed by the the fixed mirrors into two subcavities with independent optical modes a_1 and a_2 with frequency $\omega_{c,k}$ $(k = 1,2)$ and decay rate κ_k. The left fixed mirror is simultaneously driven by a strong coupling field $E_1 = \sqrt{2P_1\kappa_1/\hbar\omega_1}$ (the left coupling field) with frequency ω_1 and a weak probe field $E_p = \sqrt{2P_p\kappa_1/\hbar\omega_p}$ with frequency ω_p, in which P_l $(l = 1, p)$ denotes its power. The right subcavity is driven by another strong coupling field $E_2 = \sqrt{2P_2\kappa_2/\hbar\omega_2}$ (the right coupling field) with frequency ω_2 and power P_2. In the present paper, we focus on the optical response of the probe field to the quadratic interaction by the pressure radiations in the two-cavity optomechanical system, so we shall neglect the linear coupling between the cavity field and the membrane displacement by assuming that the membrane center-of-mass position is located exactly at a node or at an antinode of the cavity modes [41]. Then, the Hamiltonian of the double quadratically coupled optomechanical cavities is given by [40–42]

$$\begin{aligned} H = & \sum_{k=1,2} \hbar\Delta_k a_k^\dagger a_k + \frac{p^2}{2m} + \frac{1}{2}m\omega_m^2 q^2 \\ & + \hbar(g_1 a_1^\dagger a_1 - g_2 a_2^\dagger a_2)q^2 + \sum_{j=1,2} i\hbar E_j(a_j^\dagger - a_j) \\ & + i\hbar E_p(a_1^\dagger e^{-i\delta t} - a_1 e^{i\delta t}), \end{aligned} \tag{1}$$

where $\Delta_k = \omega_{c,k} - \omega_k$ $(k = 1,2)$ is the detunings between the cavity and the corresponding coupling field, and $\delta = \omega_p - \omega_1$

denotes the detuning between the left coupling field and the probe field. The momentum and displacement operators of the membrane with frequency ω_m and a mass m are denoted by p and q, respectively.

In Eq. (1), the first term denotes the free energy of the two optical cavities, and the free energy of the membrane is given by the second and third terms. The applications of the left and right coupling fields on the two fixed mirrors are given by the second summation term, and the last term describes the driving of the probe field on the left fixed mirror. The quadratic couplings between the membrane and the optical subcavities are given by the fourth term, in which the quadratic coupling coefficient is given by $g_k = \frac{8\pi^2 c}{\lambda_k^2 L_k}\sqrt{\frac{R}{1-R}}$ $(k = 1,2)$ [41,42,48,49]. Here, c is the speed of light in a vacuum, R denotes the reflectivity of the membrane, and λ_k the wavelength of the coupling field. It has been shown that the quadratic optomechanical coupling constant remarkably increases with the membrane reflectivity [41]; thus the membrane is assumed in the limit of high reflectivity to achieve the considerable quadratical interactions. The term with $\hbar g_1 a_1^\dagger a_1 q^2$ in Eq. (1), which provides a positive frequency of the movable mirror, can be realized by placing the membrane center at a node of the left subcavity field, while the membrane center is located at an antinode of the right subcavity field to achieve the contribution of a negative frequency to the membrane, i.e., $-\hbar g_2 a_2^\dagger a_2 q^2$ [27]. The system shown by the Hamiltonian in Eq. (1) is used to investigate the optomechanical trapping and the dynamics of the membrane [41,42]. Recently, the interference, entanglement, and correlation in the multimode strong-coupling optomechanics via quadratic optomechanical interactions with the same or opposite signs have been studied [40].

To consider the case in which the two cavities in the double quadratically coupled optomechanical system interact with a common reservoir besides with their respective reservoirs, we use the standard master equation approach to describe the dynamics for the membrane and the cavity variables. By tracing over the reservoir freedoms under the Born-Markov approximation, the master equation of the reduced density for the double quadratically coupled optomechanical cavities is given by

$$\begin{aligned}\frac{d\rho}{dt} = &-\frac{i}{\hbar}[H,\rho] + \sum_{i=1,2}\kappa_i(2a_i\rho a_i^\dagger - a_i^\dagger a_i\rho - \rho a_i^\dagger a_i)\\ &+ \sum_{i,j=1,2(i\neq j)}\kappa_{ij}(a_i\rho a_j^\dagger + a_j\rho a_i^\dagger - \rho a_j^\dagger a_i - a_i^\dagger a_j\rho)\\ &- \gamma_m(i[q_m,\{p_m,\rho\}] + (2n+1)[q_m,[q_m,\rho]]),\end{aligned} \tag{2}$$

where the normalized displacement and momentum operators of the mechanical oscillator are given by $q_m = \sqrt{m\omega_m/\hbar}q$ and $p_m = \sqrt{1/\hbar m\omega_m}p$ with the commutation relation $[q_m, p_m] = i$, and [...] and {...} denote commutator and anticommutator, respectively. The terms with κ_1 and κ_2 in Eq. (2) describe the individual dissipation of the cavities. And the terms with κ_{12} and κ_{21}, which are named as cross decays in the later discussions, represent a communication channel between the cavities mediated by the common reservoir, through which the cavity field loses excitation to the other cavity. This cross decay channel can be realized by placing the cavities as close as possible to each other, or by making the distance between the cavities smaller than the mode's wavelength [44]. The last term describes the excitation loss of the mechanical oscillator to its reservoir.

By using the expectation value expression $\langle X\rangle = \mathrm{Tr}(\rho X)$ and the factorization assumption $\langle AB\rangle = \langle A\rangle\langle B\rangle$, the dynamics of the system can be described by the time evolution of the expectation values for the variables, which are given by

$$\begin{aligned}\frac{d\langle a_1\rangle}{dt} &= -i(\Delta_1 + g_1\langle q^2\rangle)\langle a_1\rangle + (E_1 + E_p e^{-i\delta t})\\ &\quad - \kappa_1\langle a_1\rangle - \kappa_{12}\langle a_2\rangle, \end{aligned}\tag{3a}$$

$$\frac{d\langle a_2\rangle}{dt} = -i(\Delta_2 - g_2\langle q^2\rangle)\langle a_2\rangle + E_2 - \kappa_2\langle a_2\rangle - \kappa_{12}\langle a_1\rangle, \tag{3b}$$

$$\frac{d\langle q^2\rangle}{dt} = \frac{1}{m}\langle qp + pq\rangle, \tag{3c}$$

$$\begin{aligned}\frac{d\langle pq+qp\rangle}{dt} &= \frac{2}{m}\langle p^2\rangle - 2m\omega_m^2\langle q^2\rangle - 4\hbar(g_1\langle a_1^\dagger\rangle\langle a_1\rangle\\ &\quad - g_2\langle a_2^\dagger\rangle\langle a_2\rangle)\langle q^2\rangle - \gamma_m\langle pq+qp\rangle,\end{aligned}\tag{3d}$$

$$\begin{aligned}\frac{d\langle p^2\rangle}{dt} &= -\left[m\omega_m^2 + 2\hbar(g_1\langle a_1^\dagger\rangle\langle a_1\rangle - g_2\langle a_2^\dagger\rangle\langle a_2\rangle)\right]\\ &\quad \times\langle pq+qp\rangle - 2\gamma_m\langle p^2\rangle + 2\gamma_m(1+2n)\frac{m\hbar\omega_m}{2}.\end{aligned}\tag{3e}$$

In Eq. (3e), the last term results from the coupling of the membrane to the thermal environment, and $n = (e^{\frac{\hbar\omega_m}{\kappa_B T}} - 1)^{-1}$ is the mean thermal photon occupation number of energy $\hbar\omega_m$ at environment temperature T, in which κ_B is Boltzmann's constant and γ_m the damping rate of the membrane. The terms describing the input vacuum noise for the subcavities and the Langevin force for the membrane disappear due to their zero mean values.

Here, the coupling fields are much stronger than the probe field, and we can use the linearization approach of quantum optics to get an analytical understanding. The variables of the membrane and the cavities are divided into the steady parts and the fluctuation ones:

$$\begin{aligned} a_1 &= a_{s,1} + \delta a_1,\\ a_2 &= a_{s,2} + \delta a_2,\\ qp + pq &= (qp+pq)_s + \delta(qp+pq) = A_s + \delta_A,\\ p^2 &= (p^2)_s + \delta(p^2) = P_s + \delta P,\\ q^2 &= (q^2)_s + \delta(q^2) = Q_s + \delta Q,\end{aligned}\tag{4}$$

where we redefine the variables as $qp + pq = A$, $p^2 = P$, and $q^2 = Q$. Substituting Eq. (4) into Eqs. (3a)–(3e) and setting all the time derivations to be zero, the steady-state solutions, which are mainly determined by the strong coupling fields, are

obtained as

$$\begin{aligned} a_{s,1} &= \frac{E_1(\kappa_2 + i\Delta_2') - \kappa_{12}E_2}{(\kappa_1 + i\Delta_1')(\kappa_2 + i\Delta_2') - \kappa_{12}\kappa_{21}}, \\ a_{s,2} &= \frac{E_2(\kappa_1 + i\Delta_1') - \kappa_{21}E_1}{(\kappa_1 + i\Delta_1')(\kappa_2 + i\Delta_2') - \kappa_{12}\kappa_{21}}, \\ A_s &= 0, \\ P_s &= m\hbar\omega_m\left(n + \frac{1}{2}\right), \\ Q_s &= \frac{P_s}{m^2\omega_m^2 + 2m\hbar(g_1 a_{s,1}^* a_{s,1} - g_2 a_{s,2}^* a_{s,2})}, \end{aligned} \tag{5}$$

where $\Delta_1' = \Delta_1 + g_1 Q_s$ and $\Delta_2' = \Delta_2 - g_2 Q_s$ are the effective cavity detunings, in which the radiation pressure effects induced by the coupling fields produce opposite contributions to the corresponding detunings. It is shown from Eq. (5) that the steady kinetic energy $\frac{P_s}{2m}$ of the membrane is mainly contributed from thermal photons of the environment, and the potential energy $m\omega_m^2 Q_s/2$ is dependent on the two coupling powers besides on the thermal photons. The dependence of the physics processes on the thermal photons and the temperature of the environment comes from the two-phonon process shown in Eq. (1). It is noted that the mean value of the displacement for the quadratically coupled membranes is zero; this is different from the case of the linear optomechanical coupling where the mean value of the displacement is not zero and determines the steady intracavity field [13]. Physically, in the case of the linear coupling the radiation pressure gives a force upon the mechanical resonator and displaces the oscillator to a new equilibrium position. However, the steady-state intracavity field $a_{s,k}$ ($k = 1,2$) in Eq. (5) is independent of the quadratic coupling constant $g_{s,k}$; thus the quadratic coupling from the radiation pressure will not affect the displacement of the membrane through intercavity fields but change the resonant frequency of the mechanical resonator, and the thermal photons of the environment on average have no effects on the motion of the mechanical resonator.

Correspondingly, the time evolution for the expectation values of the fluctuations is given by

$$\begin{aligned} \frac{d\langle\delta a_1\rangle}{dt} &= -(\kappa_1 + i\Delta_1')\langle\delta a_1\rangle - i a_{s,1} g_1 \langle\delta Q\rangle \\ &\quad + E_p e^{-i\delta t} - \Gamma_C\langle\delta a_2\rangle, \end{aligned} \tag{6}$$

$$\begin{aligned} \frac{d\langle\delta a_2\rangle}{dt} &= -(\kappa_2 + i\Delta_2')\langle\delta a_2\rangle + i a_{s,2} g_2 \langle\delta Q\rangle \\ &\quad - \Gamma_C\langle\delta a_1\rangle, \end{aligned} \tag{7}$$

$$\frac{d\langle\delta Q\rangle}{dt} = \frac{1}{m}\langle\delta A\rangle, \tag{8}$$

$$\begin{aligned} \frac{d\langle\delta A\rangle}{dt} &= \frac{2}{m}\langle\delta P\rangle - 2m\omega_m^2\langle\delta Q\rangle \\ &\quad - 4\hbar\{(g_1 a_{s,1}^* a_{s,1} - g_2 a_{s,2}^* a_{s,2})\langle\delta Q\rangle \\ &\quad + Q_s[g_1(a_{s,1}^*\langle\delta a_1\rangle + a_{s,1}\langle\delta a_1^\dagger\rangle) \\ &\quad - g_2(a_{s,2}^*\langle\delta a_2\rangle + a_{s,2}\langle\delta a_2^\dagger\rangle)]\} \\ &\quad - \gamma_m\langle\delta A\rangle, \end{aligned} \tag{9}$$

$$\begin{aligned} \frac{d\langle\delta P\rangle}{dt} &= -\left[m\omega_m^2 + 2\hbar(g_1 a_{s,1}^* a_{s,1} - g_2 a_{s,2}^* a_{s,2})\right]\langle\delta A\rangle \\ &\quad - 2\gamma_m\langle\delta P\rangle, \end{aligned} \tag{10}$$

where the cross-decay rates are assumed to be equal to each other, i.e., $\kappa_{12} = \kappa_{21} = \Gamma_C$. In order to display the probe optical properties, we make these *Ansätze* as follows:

$$\begin{aligned} \langle\delta Q\rangle &= Q_+ e^{-i\delta t} + Q_- e^{i\delta t}, \\ \langle\delta A\rangle &= A_+ e^{-i\delta t} + A_- e^{i\delta t}, \\ \langle\delta P\rangle &= P_+ e^{-i\delta t} + P_- e^{i\delta t}, \\ \langle\delta a_1\rangle &= a_{1+} e^{-i\delta t} + a_{1-} e^{i\delta t}, \\ \langle\delta a_2\rangle &= a_{2+} e^{-i\delta t} + a_{2-} e^{i\delta t}. \end{aligned} \tag{11}$$

Substituting these *Ansätze* into Eqs. (6)–(10), we obtain the following expression:

$$\begin{aligned} a_{1+} &= \frac{a_{s1} g_1(\delta - \Delta_2') + i(a_{s1} g_1 \kappa_2 + a_{s2} g_2 \Gamma_C)}{\Omega_1} Q_+ \\ &\quad + \frac{i E_p(\delta - \Delta_2') - \kappa_2 E_p}{\Omega_1}, \end{aligned} \tag{12}$$

where

$$Q_+ = \frac{\Omega_2\Omega_3\Phi_2}{\Omega_1\Omega_2\Phi_4 - \Omega_1\Omega_3\Phi_1 - \Omega_2\Omega_3\Phi_3}, \tag{13}$$

with

$$\begin{aligned} \Omega_1 &= \left[(\delta - \Delta_2')(\delta - \Delta_1') - \kappa_1\kappa_2 + \Gamma_C^2\right] \\ &\quad + i[(\delta - \Delta_2')\kappa_1 + (\delta - \Delta_1')\kappa_2], \end{aligned} \tag{14}$$

$$\begin{aligned} \Omega_2 &= \left[(\delta + \Delta_2')(\delta + \Delta_1') - \kappa_1\kappa_2 + \Gamma_C^2\right] \\ &\quad + i[(\delta + \Delta_2')\kappa_1 + (\delta + \Delta_1')\kappa_2], \end{aligned} \tag{15}$$

$$\Omega_3 = \delta + 2i\gamma_m, \tag{16}$$

$$\begin{aligned} \Phi_1 &= 4m\hbar Q_s\left[a_{s2}^2 g_2^2(\delta + \Delta_1') + a_{s1}^2 g_1^2(\delta + \Delta_2')\right] \\ &\quad + 4im\hbar Q_s\left(a_{s2}^2 g_2^2\kappa_1 + a_{s1}^2 g_1^2\kappa_2 + 2a_{s1}a_{s2}g_1g_2\Gamma_C\right), \end{aligned} \tag{17}$$

$$\begin{aligned} \Phi_2 &= 4m\hbar Q_s E_p(a_{s1}^* g_1\kappa_2 + a_{s2}^* g_2\Gamma_C) \\ &\quad - 4im\hbar Q_s E_p a_{s1}^* g_1(\delta - \Delta_2'), \end{aligned} \tag{18}$$

$$\begin{aligned} \Phi_3 &= -4m\hbar Q_s\left[a_{s1}a_{s1}^* g_1^2(\delta - \Delta_2') + a_{s2}a_{s2}^* g_2^2(\delta - \Delta_1')\right] \\ &\quad - 4im\hbar Q_s[a_{s1}g_1(a_{s1}^* g_1\kappa_2 + a_{s2}^* g_2\Gamma_C) \\ &\quad + a_{s2}g_2(a_{s1}^* g_1\Gamma_C + a_{s2}^* g_2\kappa_1)], \end{aligned} \tag{19}$$

$$\begin{aligned} \Phi_4 &= 8m\hbar\delta\left(a_{s1}a_{s1}^* g_1 - a_{s2}a_{s2}^* g_2^2\right) + m^2\delta\left(4\omega_m^2 - \delta^2\right) \\ &\quad + 2m^2\gamma_m^2\delta + i\left[8m\hbar\gamma_m(a_{s1}a_{s1}^* g_1 - a_{s2}a_{s2}^* g_2)\right. \\ &\quad \left. + m^2\gamma_m\left(4\omega_m^2 - \delta^2\right) - 2m^2\gamma_m\delta^2\right]. \end{aligned} \tag{20}$$

Further, the output field can be derived by using the input-output relation

$$\varepsilon_{\text{out}}(t) = \varepsilon_{\text{out}0} + \varepsilon_{\text{out}+} e^{-i\delta t} + \varepsilon_{\text{out}-} e^{i\delta t}. \tag{21}$$

The probe response to the system can be described by the component of the output field $\varepsilon_{\text{out}+} = 2\kappa_1 a_{1+}/E_p$ [13,14,48], which oscillates at the probe frequency ω_p. And the probe absorption properties of the system are given by the real part of the output field $\varepsilon_R = \text{Re}[\varepsilon_{\text{out}+}]$.

III. OMIT AS WELL AS ITS VARIATIONS WITH COUPLING FIELDS

In this section, we shall focus on the dependence of the OMIT in the double quadratically coupled optomechanical cavities on the two coupling fields as well as their intensity difference. The influence of the cross decay on the OMIT will be discussed in the next section. In order to numerically analyze the transparency of the probe field in the quadratically coupled double-cavity optomechanical system, we use the parameters in Ref. [48]: $\omega_{c1} = \omega_{c2} = 1.77 \times 10^{12}$ Hz, $\kappa_1 = \kappa_2 = 2\pi \times 10^4$ Hz, $\gamma_m = 2 \times 10$ Hz, $\omega_m = 2\pi \times 10^5$ Hz, $m = 1 \times 10^{-12}$ kg, and $L_1 = 6.7 \times 10^{-2}$ m. Here, the wavelengths of the left and right coupling fields are given by $\lambda_1 = 532 \times 10^{-9}$ m [48] and $\lambda_2 = 514 \times 10^{-9}$ m [41], respectively. Without loss of generality, the two quadratic coupling coefficients are assumed to be equal, $g_1 = g_2$, by setting the subcavity lengths and the wavelengths of the two coupling fields to follow the relation $\lambda_1^2 L_1 = \lambda_2^2 L_2$. At the same time, to display the effects of the the intensity difference between the coupling fields on OMIT we set the ratio of the right coupling intensity to the left one as $n = |E_2|^2/|E_1|^2 = P_2\lambda_2/P_1\lambda_1$. The following discussions are developed under the two-phonon resonance, i.e., $\Delta_1' = \Delta_2' = 2\omega_m$, and the detuning between the left coupling and probe fields is redefined by $\sigma = (\delta - 2\omega_m)/\omega_m$ to display the probe transparency properties around the two-phonon resonance.

First, we investigate the effects of the left coupling field $|E_1|^2$ on the probe absorption properties in the system. In Fig. 2, the right coupling field is fixed at $P_2 = 20.70$ μW, and the left coupling field is given by $P_1 = 4$ μW, 20 μW, and 36 μW, which are shown by the solid, dashed, and dotted curves, respectively. We find that there appears a narrow transparency dip located at $\sigma = -0.01\omega_m$, 0, and $0.01\omega_m$ for $P_1 = 4$ μW, 20 μW, and 36 μW, and the transparency dip becomes deeper and wider with increase of the left coupling intensity. Also, it is shown that the transparency positions for $P_1 = 4$ μW and 36 μW are located symmetrically about the resonant point due to their identical intensity differences between the left and right coupling fields with opposite signs, and the transparency position for $P_1 = 20$ μW lies at the resonant point because of the identical intensities for the two coupling fields, i.e., $|E_1|^2 = |E_2|^2$. The extremely narrow nature with the transparency dip is due to $\gamma_m \ll \kappa_i$ $(i = 1,2)$. Additionally, it is shown that when increasing the intensity of the left coupling field, the transparency dip will be shifted to high frequency. This is because the quadratic optomechanical interaction induced by the left coupling field provides a positive contribution to the membrane frequency.

Now we consider the influences of the right coupling field on the probe transparency spectrum by setting the right coupling field with different values. It is shown in Fig. 3 with the left coupling field fixed at $P_1 = 20$ μW that the transparency dip is located at $\sigma = -0.01\omega_m$, 0,

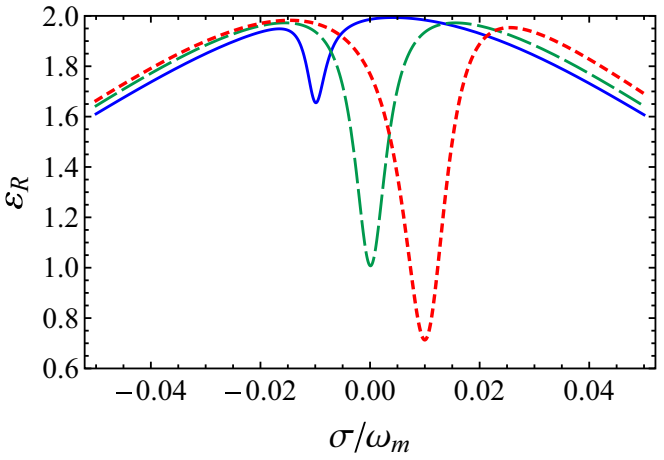

FIG. 2. The probe absorption ε_R versus the normalized detuning σ/ω_m with the right coupling field fixed at $P_2 = 20.70$ μW, and the power of the left coupling field is given by different values: $P_1 = 4$ μW (blue, solid curve); $P_1 = 20$ μW (green, dashed curve); $P_1 = 36$ μW (red, dotted curve). The other values of the parameters are given by $\omega_{c1} = \omega_{c2} = 1.77 \times 10^{12}$ Hz, $\kappa_1 = \kappa_2 = 2\pi \times 10^4$ Hz, $\kappa_{12} = \kappa_{21} = 0$, $\gamma_m = 2 \times 10$ Hz, $\omega_m = 2\pi \times 10^5$ Hz, $m = 1 \times 10^{-12}$ kg, $L_1 = 6.7 \times 10^{-2}$ m, $\lambda_1 = 532 \times 10^{-9}$ m, $\lambda_2 = 514 \times 10^{-9}$ m, $R = 0.95$, and $T = 90$ K. To meet the situation of the identical quadratic coupling coefficients, i.e., $g_1 = g_2$, the subcavity lengths and the wavelengths of the two coupling fields obey the relation $\lambda_1^2 L_1 = \lambda_2^2 L_2$.

and $0.01\omega_m$ for $P_1 = 37.26$ μW, 20.07 μW, and 4.14 μW, and the transparency dip becomes shallower with stronger right coupling field. Additionally, the transparency position is shifted to lower frequency with increase of the right coupling field. The situation is contrary to the case for the left coupling field shown in Fig. 2. This can be understood by the quadratical couplings between the subcavity fields and the membrane in Eq. (1): the left coupling field induces a

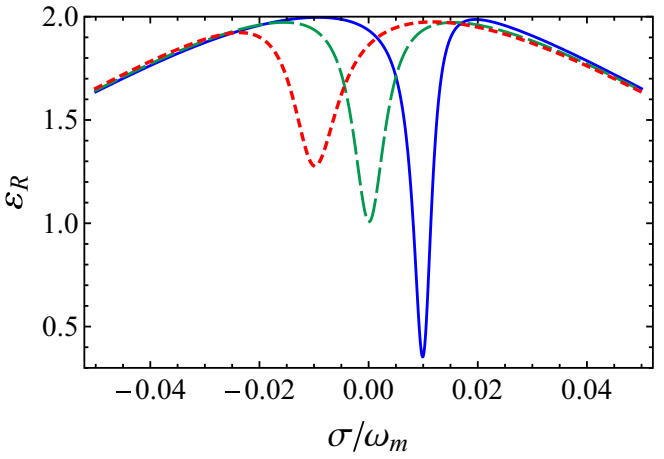

FIG. 3. The probe absorption ε_R versus the normalized detuning σ/ω_m with $P_1 = 20$ μW and with different right coupling intensities: $P_2 = 4.14$ μW (blue, solid curve); $P_2 = 20.70$ μW (green, dashed curve); $P_2 = 37.26$ μW (red, dotted curve). The other values of the parameters are the same as in Fig. 2.

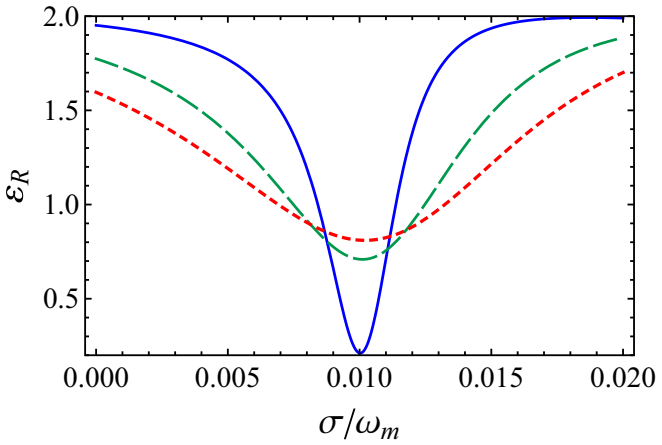

FIG. 4. The probe absorption ε_R versus the normalized detuning σ/ω_m with different powers of the left and the right coupling field: $P_1 = 18\ \mu$W, $P_2 = 1.86\ \mu$W (blue, solid curve); $P_1 = 36\ \mu$W, $P_2 = 20.5\ \mu$W (green, dashed curve); $P_1 = 52\ \mu$W, $P_2 = 37.05\ \mu$W (red, dotted curve). The intensity differences between the two coupling fields in these three settings are identical, i.e., $\Delta I = |E_2|^2 - |E_1|^2 \approx 8.62 \times 10^{-12}\xi$ with $\xi = \kappa/\pi c\hbar$. Other values of the parameters are the same as in Fig. 2.

positive quadratical coupling and then increases the effective frequency of the left subcavity, while the right coupling field results in a negative one and decreases the right subcavity's effective frequency. Correspondingly, this will shift the probe transparency frequency, which is resonant with the cavity's frequency.

In the above discussions, we consider the effects of one coupling field on the probe absorption properties by fixing the other coupling field. Now we shall investigate the behaviors of the system in the case in which the two coupling fields are both varying while their intensity difference is kept unchanged. In Fig. 4, we increase the powers of the two coupling fields while fixing their intensity differences at $\Delta I = |E_2|^2 - |E_1|^2 \approx 8.62 \times 10^{-12}\xi$ with $\xi = \kappa/\pi c\hbar$. It is shown that the transparency window becomes shallower and wider with increase of the coupling fields, and the transparency positions in these cases are located exactly at $\sigma = 0.01\omega_m$. This further proves that the transparency position is determined by the intensity difference between the two coupling fields. From the expression of the output field in Eq. (12), we get the analytical findings for the transparency position:

$$\sigma_t/\omega_m = 2\hbar(g_1 a_{s,1}^* a_{s,1} - g_2 a_{s,2}^* a_{s,2})/m\omega_m^2. \tag{22}$$

We can see that the left coupling field provides a positive value to the normalized detuning through the left intracavity field while the right coupling field leads to the negative value through the right intracavity field. This explains why the transparency window shifts to the high frequency with increase of the left coupling field, while the right coupling field leads to the opposite shift. Thus the scheme in the present paper can solve the problem of the transparency frequency shift in general single-mode quadratically coupled optomechanical system. Now we can investigate how the probe maximal transparency varies with the coupling fields in terms of the the analytical findings. We plot the probe absorptions

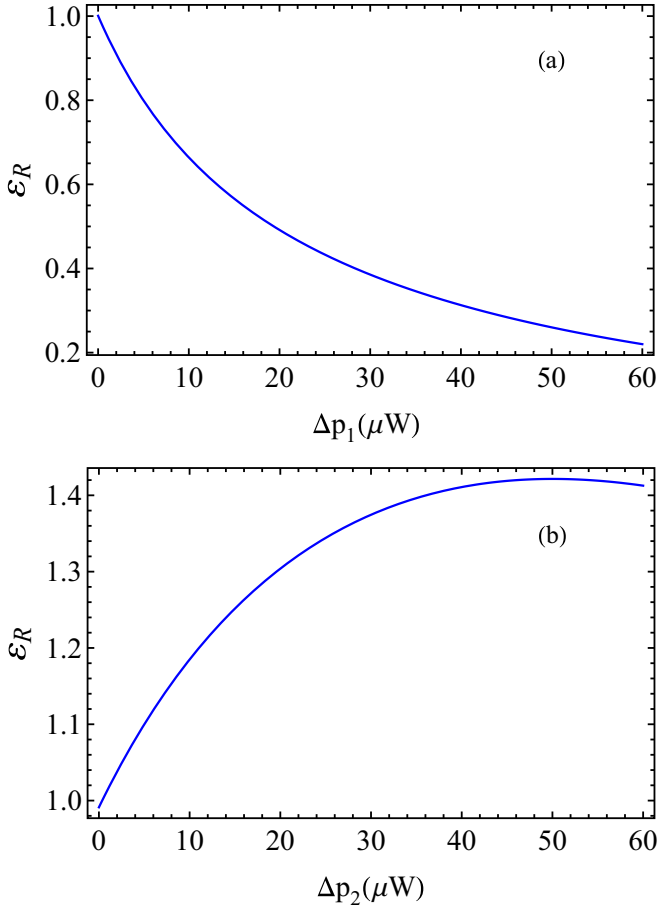

FIG. 5. The probe absorption ε_R at the transparent position $\sigma_t/\omega_m = 2\hbar(g_1 a_{s,1}^* a_{s,1} - g_2 a_{s,2}^* a_{s,2})/m\omega_m^2$ versus the power difference: (a) $\Delta_{p1} = P_1 - P_2$, $P_2 = 20\ \mu$W; (b) $\Delta_{p2} = P_2 - P_1$, $P_1 = 20\ \mu$W. Other values of the parameters are the same as in Fig. 2.

at the transparency position σ_t versus the power difference between the left and the right coupling fields in Fig. 5(a) for $\Delta_{P1} = P_1 - P_2$ with $P_1 = 20\ \mu$W, and in Fig. 5(b) for $\Delta_{P2} = P_2 - P_1$ with $P_2 = 20\ \mu$W. It is shown from Fig. 5(a) that when the left coupling field is stronger than the right one the maximal transparency in the probe absorption spectrum becomes enhanced. However, the maximal transparency is suppressed for the case where the right coupling field is stronger than the left one, which is shown by Fig. 5(b).

IV. ENHANCED OMIT BY THE CROSS DECAY INDUCED BY A COMMON RESERVOIR

In the previous section, we consider the variation of the OMIT with two coupling fields in the case where two subcavities of the system are only interacting with their respective reservoirs. Now, we shall investigate the OMIT in the present system in which two subcavities are coupling with a common reservoir, and explore the effects of the cross decay induced by the common reservoir on the OMIT. Without loss of generality, it is assumed that the decay rates for the two cavities are identical, i.e., $\kappa_1 = \kappa_2$, the two cavities are in the resonant condition, i.e., $\omega_{c1} = \omega_{c2}$, and the cross decays κ_{12} and κ_{21} can be set to be identical and can be expressed

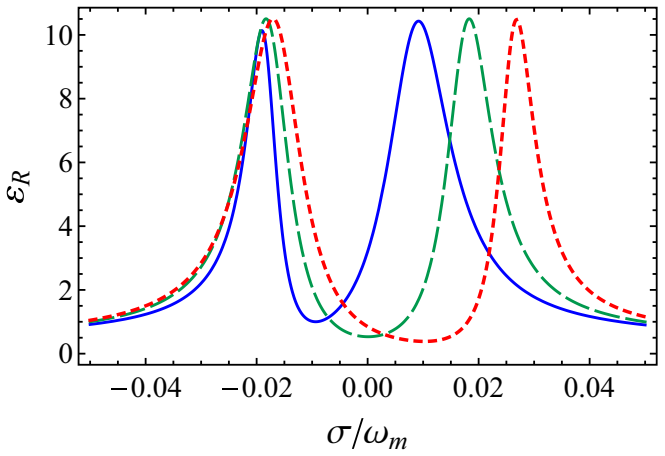

FIG. 6. The same settings are used as in Fig. 2, but for $\eta = 0.9$ with the definition of $\Gamma_C = \kappa_{12} = \kappa_{21} = \eta\sqrt{\kappa_1\kappa_2}$.

by $\kappa_{12} = \kappa_{21} = \eta\sqrt{\kappa_1\kappa_2}$, with $\eta \in [0,1]$ being the coupling efficiency between the cavities through the common reservoir [50]. It was shown that the cross decay can be adjusted through the engineered reservoirs [43].

First, we consider the variation of the OMIT with the left coupling field in the presence of the cross decay. It is shown from Fig. 6 with $\eta = 0.9$ that the three transparency positions for $P_1 = 4\ \mu$W, 20 μW, and 36 μW are still located at $\sigma = -0.01\omega_m$, 0, and $0.01\omega_m$, which is the same as those in Fig. 2. By comparing Fig. 6 with Fig. 2, we can see that the transparency window becomes intensely deeper and wider in the presence of the cross decay. The strong left coupling field leads to a remarkable blueshift of the right absorption peak in the OMIT window, while the left absorption peak has hardly changed. It is the blueshift that makes the transparency window wider. The increase of the maximal transparency with the left coupling field can be seen in Fig. 6, but with a slighter strength than Fig. 2. Correspondingly, the variation of the OMIT with the right coupling filed in the presence of the cross decay is shown in Fig. 7. It is also shown that the transparency window becomes deeper and wider than those in

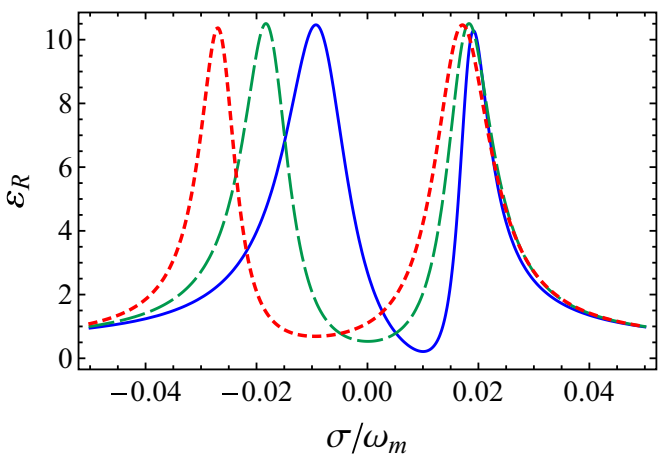

FIG. 7. The same settings are used as in Fig. 3, but for $\eta = 0.9$ with the definition of $\Gamma_C = \kappa_{12} = \kappa_{21} = \eta\sqrt{\kappa_1\kappa_2}$.

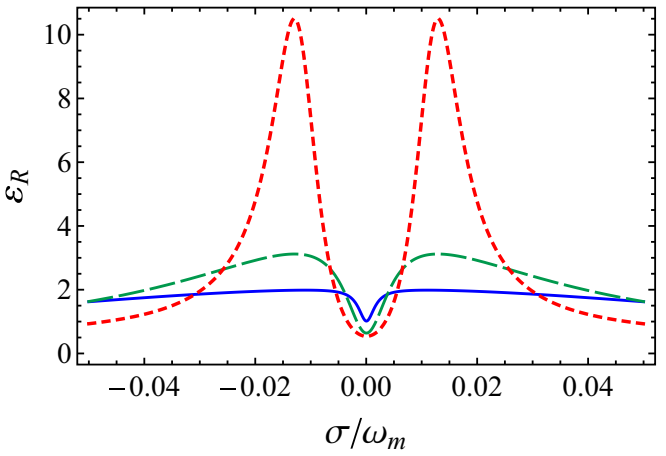

FIG. 8. The probe absorption ε_R versus the normalized detuning σ/ω_m with $P_1 = 20\ \mu$W and $n = 1$ ($|E_2|^2 = |E_1|^2$) for the different cross decays ($\kappa_{12} = \kappa_{21} = \eta\sqrt{\kappa_1\kappa_2}$): $\eta = 0$ (blue, solid curve); $\eta = 0.6$ (green, dashed curve); $\eta = 0.9$ (red, dotted curve). Other values of the parameters are the same as in Fig. 2.

the absence of the cross decay shown in Fig. 3. At this time, the wider transparency window comes from the redshift of the left absorption peak, which is induced by the right coupling field. The blueshifts or redshifts of the absorption peaks in the OMIT window can be used to distinguish between the left and right coupling fields.

Second, we shall investigate the effects of the cross decay on the OMIT when the two coupling fields are kept unchanged with identical intensity. This situation is shown by Fig. 8 with different cross decays by setting the coupling efficiency as $\eta = 0, 0.6, 0.9$, which correspond to solid, dashed, and dotted curves. It is shown that the maximal transparency for $\eta = 0.6$, shown by the dashed curve, becomes larger than the solid curve in the absence of the cross decay. If the cross decay increases up to $\eta = 0.9$, the transparency window gets wider and its transparency window becomes ten times deeper than the solid curve.

Although the OMIT in the present system is improved by the left coupling field, the transparency position will move with its varying intensity. How do we make the probe field transparent to be fixed at a certain frequency ω_x? From the above discussions, we can see that the transparency position can be fixed by additionally using the right coupling field to meet the relation $2\hbar(g_1 a_{s,1}^* a_{s,1} - g_2 a_{s,2}^* a_{s,2})/m\omega_m = \omega_x$; i.e., the main function of the right coupling field is used to fix transparency frequency for the probe field. However, the right coupling field can suppress the transparency. In the present system the suppressed transparency by the right coupling field can be compensated by the cross decay induced by the common reservoir. Now we consider the effects of the cross decays on the minimum absorption at the transparency position ω_x when increasing the right coupling field. It is shown from Fig. 9 that the minimal absorption for $\eta = 0.5$ shown by the dashed curve is smaller than that shown by the solid curve with $\eta = 0$, and the absorption for $\eta = 1.0$, the decoherence-free situation in cavity quantum electrodynamics [44], is remarkably smaller than dashed curve. Thus the transparency is remarkably improved by the cross decay. Additionally, the slope of the

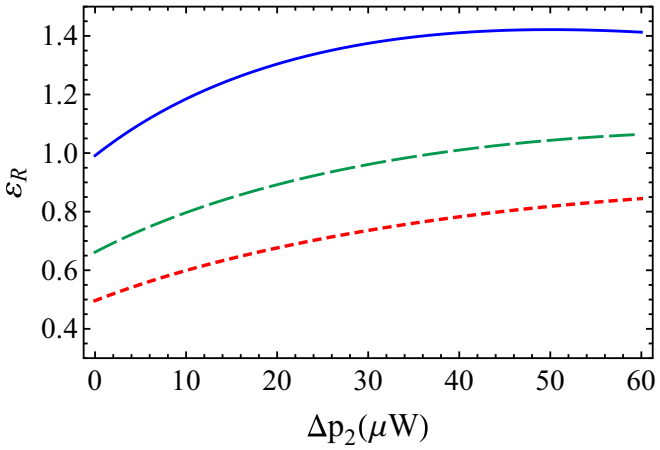

FIG. 9. The probe absorption ε_R at the transparent position $\sigma_t/\omega_m = 2\hbar(g_1 a_{s,1}^* a_{s,1} - g_2 a_{s,2}^* a_{s,2})/m\omega_m^2$ versus the coupling power difference $\Delta_{p2} = P_2 - P_1$ with $P_1 = 20\ \mu$W, and the cross decay is given by different values ($\kappa_{12} = \kappa_{21} = \eta\sqrt{\kappa_1\kappa_2}$): $\eta = 0$ (blue, solid curve); $\eta = 0.5$(green, dashed curve); $\eta = 1$ (red, dotted curve). Other values of the parameters are the same as in Fig. 2.

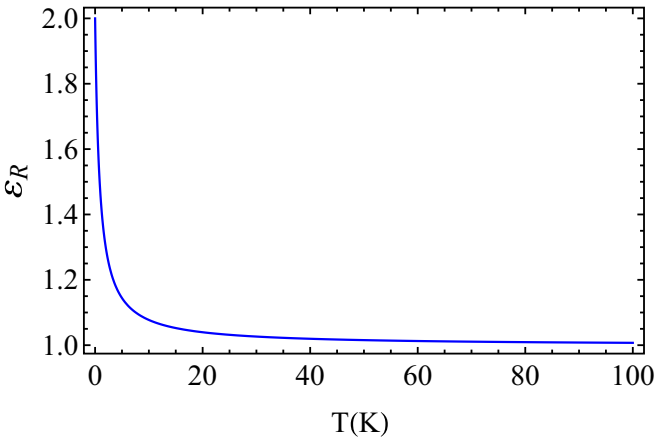

FIG. 10. The probe absorption ε_R versus the temperature of the environment T with $P_1 = 20\ \mu$W and $n = 1$ ($|E_2|^2 = |E_1|^2$). Other values of the parameters are the same as in Fig. 2.

minimum absorption curve varying with the enhanced right coupling field becomes gentler when the cross decay is increased. This implies that the cross decay can ameliorate the suppressed transparency induced by the right coupling field. It is well known that OMIT in the optomechanical system comes from the destructive interference between the probe field and the anti-Stokes field induced by the radiation pressure, and the transparency is mainly limited by the individual dissipations or the decoherences from the environments surrounding the membrane and the cavities. On the other hand, the cross decay provides a communication channel between the cavities mediated by the common reservoir, and scatters one optical mode to the other without losing their coherence. The cross decay can supply the coherence destroyed by the individual dissipation or decoherence, which explains why the cross decay can improve the OMIT.

Finally, we shall display the effects of the temperature of the environment on the OMIT. We consider the variation of the probe OMIT at the two-phonon resonance $\sigma/\omega_m = 0$ (or $\delta = 2\omega_m$) with the temperature, which is shown by Fig. 10. It is shown that the transparency is markedly improved by increasing the temperature of the environment below $T = 40$ K, beyond which the probe field is saturated. From Eq. (5), it is shown that the thermal photons of the environment are transferred to the kinetic energy of the membrane in the quadratically coupled optomechanical system. The kinetic energy enhances the oscillation of the membrane induced by the simultaneous applications of the driving fields, and can alleviate the destruction from the damping process on the OMIT. This can explain why the temperature can improve the OMIT. Recently, it has been shown that the environment temperature together with the coupling field power jointly drive the realization of slow light [49].

V. CONCLUSION

In conclusion, we have considered the OMIT in the double quadratically coupled optomechanical cavities, in which the two cavities are driven by the coupling fields. It is found that the probe transparency is improved and the transparency position (the probe frequency of the maximal transparency) is shifted to high frequency with increase of the left coupling field, while the coupling field applied on the coupled cavity can attenuate probe transparency and lead to a low-frequency shift. In fact, the transparency position is exactly determined by the intensity difference between the two coupling fields. Additionally, we have considered the OMIT in the case where the two cavities are coupled to a common reservoir. Unlike the usual dissipation into the subsystem's own reservoir, the cross decay induced by the common reservoir can improve the OMIT in the quadratically optomechanical system even if the right coupling field is stronger than the left one. Finally, the effects of the temperature of the environment on the OMIT have been investigated. This will help in cooling of the membrane, squeezing and entangling the output fields.

ACKNOWLEDGMENTS

This work was supported partly by the National Natural Science Foundation of China under Grant No. 10647007 and the Young Foundation of Sichuan Province, China, under Grant No. 09ZQ026-008.

[1] P. Meystre, Ann. Phys. **525**, 215 (2013).
[2] T. J. Kippenberg and K. J. Vahala, Opt. Express **15**, 17172 (2007).
[3] M. Aspelmeyer, T. J. Kippenberg, and F. Marquardt, Rev. Mod. Phys. **86**, 1391 (2014).

[4] D. Vitali, S. Gigan, A. Ferreira, H. R. Böhm, P. Tombesi, A. Guerreiro, V. Vedral, A. Zeilinger, and M. Aspelmeyer, Phys. Rev. Lett. **98**, 030405 (2007).

[5] J. Teufel, T. Donner, D. Li, J. W. Harlow, M. S. Allman, K. Cicak, A. J. Sirois, J. D. Whittaker, K. Lehnert, and R. Simmonds, Nature (London) **475**, 359 (2011).

[6] J. Chan, T. P. M. Alegre, A. H. Safavi Naeini, J. T. Hill, A. Krause, S. Groblacher, M. Aspelmeyer, and O. Painter, Nature (London) **478**, 89 (2011).

[7] M. Bhattacharya and P. Meystre, Phys. Rev. Lett. **99**, 073601 (2007).

[8] P. Rabl, Phys. Rev. Lett. **107**, 063601 (2011).

[9] M. Ludwig, A. H. Safavi-Naeini, O. Painter, and F. Marquardt, Phys. Rev. Lett. **109**, 063601 (2012).

[10] X.-Y. Lü, W.-M. Zhang, S. Ashhab, Y. Wu, and F. Nori, Sci. Rep. **3**, 2943 (2013).

[11] S. E. Harris, Phys. Today **50**, 36 (1997).

[12] K. J. Boller, A. Imamoğlu, and S. E. Harris, Phys. Rev. Lett. **66**, 2593 (1991).

[13] G. S. Agarwal and S. Huang, Phys. Rev. A **81**, 041803(R) (2010).

[14] S. Weis, R. Riviere, S. Deleglise, E. Gavartin, O. Arcizet, A. Schliesser, and T. J. Kippenberg, Science **330**, 1520 (2010).

[15] A. H. Safavi-Naeini, T. P. Mayer Alegre, J. Chan, M. Eichenfield, M. Winger, Q. Lin, J. T. Hill, D. Chang, and O. Painter, Nature (London) **472**, 69 (2011).

[16] H. Xiong, L.-G. Si, A.-S. Zheng, X. Yang, and Y. Wu, Phys. Rev. A **86**, 013815 (2012).

[17] M.-A. Lemonde, N. Didier, and A. A. Clerk, Phys. Rev. Lett. **111**, 053602 (2013).

[18] K. Børkje, A. Nunnenkamp, J. D. Teufel, and S. M. Girvin, Phys. Rev. Lett. **111**, 053603 (2013).

[19] A. Kronwald and F. Marquardt, Phys. Rev. Lett. **111**, 133601 (2013).

[20] S. Shahidani, M. H. Naderi, and M. Soltanolkotabi, Phys. Rev. A **88**, 053813 (2013).

[21] C. Jiang, H. Liu, Y. Cui, X. Li, G. Chen, and B. Chen, Opt. Express **21**, 12165 (2013).

[22] Kenan Qu and G. S. Agarwal, Phys. Rev. A **87**, 031802(R) (2013).

[23] J. Ma, C. You, L. Si, H. Xiong, X. Yang, and Y. Wu, Opt. Lett. **39**, 4180 (2014).

[24] B. P. Hou, L. F. Wei, and S. J. Wang, Phys. Rev. A **92**, 033829 (2015).

[25] J. D. Thompson, B. M. Zwick, A. M. Jayich, F. Marquardt, S. M. Girvin, and J. G. E. Harris, Nature (London) **452**, 72 (2008).

[26] J. C. Sankey, C. Yang, B. M. Zwickl, A. M. Jayich, and J. G. E. Harris, Nat. Phys. **6**, 707 (2010).

[27] M. Karuza, M. Galassi, C. Biancofiore, C. Molinelli, R. Natali, P. Tombesi, G. Di Giuseppe, and D. Vitali, J. Opt. **15**, 025704 (2013).

[28] A. Nunnenkamp, K. Børkje, J. G. E. Harris, and S. M. Girvin, Phys. Rev. A **82**, 021806(R) (2010).

[29] M. Asjad, G. S. Agarwal, M. S. Kim, P. Tombesi, G. Di. Giuseppe, and D. Vitali, Phys. Rev. A **89**, 023849 (2014).

[30] O. Romero-Isart, A. C. Pflanzer, F. Blaser, R. Kaltenbaek, N. Kiesel, M. Aspelmeyer, and J. I. Cirac, Phys. Rev. Lett. **107**, 020405 (2011).

[31] H. Shi and M. Bhattacharya, Phys. Rev. A **87**, 043829 (2013).

[32] H. Tan, F. Bariani, G. Li, and P. Meystre, Phys. Rev. A **88**, 023817 (2013).

[33] L. F. Buchmann, L. Zhang, A. Chiruvelli, and P. Meystre, Phys. Rev. Lett. **108**, 210403 (2012).

[34] J.-Q. Liao and F. Nori, Sci. Rep. **4**, 6302 (2014).

[35] T. P. Purdy, D. W. C. Brooks, T. Botter, N. Brahms, Z.-Y. Ma, and D. M. Stamper-Kurn, Phys. Rev. Lett. **105**, 133602 (2010).

[36] J.-Q. Liao and F. Nori, Phys. Rev. A **88**, 023853 (2013).

[37] A. B. Shkarin, N. E. Flowers-Jacobs, S. W. Hoch, A. D. Kashkanova, C. Deutsch, J. Reichel, and J. G. E. Harris, Phys. Rev. Lett. **112**, 013602 (2014).

[38] M. Bhattacharya and P. Meystre, Phys. Rev. A **78**, 041801(R) (2008).

[39] X.-W. Xu, Y.-J. Zhao, and Y.-x. Liu, Phys. Rev. A **88**, 022325 (2013).

[40] H. Seok, L. F. Buchmann, E. M. Wright, and P. Meystre, Phys. Rev. A **88**, 063850 (2013).

[41] M. Bhattacharya, H. Uys, and P. Meystre, Phys. Rev. A **77**, 033819 (2008).

[42] J. H. Teng, S. L. Wu, B. Cui, and X. X. Yi, J. Phys. B **45**, 185506 (2012).

[43] M. A. de Ponte, M. C. de Oliveira, and M. H. Y. Moussa, Ann. Phys. **317**, 72 (2005).

[44] A. R. Bosco de Magalhães and M. C. Nemes, Phys. Rev. A **70**, 053825 (2004).

[45] J. P. Paz and A. J. Roncaglia, Phys. Rev. Lett. **100**, 220401 (2008).

[46] G. Manzano, F. Galve, G. L. Giorgi, E. Hernández-García, and R. Zambrini, Sci. Rep. **3**, 1439 (2013).

[47] A. Xuereb, A. Imparato, and A. Dantan, New J. Phys. **17**, 055013 (2015).

[48] Sumei Huang and G. S. Agarwal, Phys. Rev. A **83**, 023802 (2011).

[49] X.-G. Zhan, L.-G. Si, A.-S. Zheng, and X. Yang, J. Phys. B **46**, 025501 (2013).

[50] A. S. Parkins, E. Solano, and J. I. Cirac, Phys. Rev. Lett. **96**, 053602 (2006).